Band-theory description of high-energy spectroscopy and the electronic structure of $LiCoO_2$

M. T. Czyżyk, R. Potze, and G. A. Sawatzky
Department of Solid State and Applied Physics, University of Groningen, Nijenborgh 18, NL-9747 AG Groningen, The Netherlands
(Received 19 November 1991)

$LiCoO_2$ can be viewed as the end member of the Li-doped $Li_xCo_{1-x}O_2$ system. It was suggested that this system exhibits a transition from high-spin Co ions in CoO to low-spin Co ions in $LiCoO_2$. We present a systematic study of the electronic properties of $LiCoO_2$ based on a density-functional calculation. From a good agreement between the theoretical results and the results of various spectroscopies (x-ray photoemission spectroscopy, bremsstrahlung isochromat spectroscopy, and x-ray absorption spectroscopy) we conclude that a one-particle band-structure approach is basically adequate for $LiCoO_2$ (while being still controversial for CoO) and we support the conclusion of low-spin Co ions in this compound.

I. INTRODUCTION

Transition metal (TM) oxides have attracted a lot of attention for a long time.[1,2] The dispute about the nature of their electronic structure is widely documented in the literature,[1-6] reflecting the evolution of opinions about whether the gap is a Mott-Hubbard or a charge-transfer one. The interest in TM oxides was reignited in recent years by the discovery of high-T_c superconductors. The late TM monoxides can be doped with Li, forming $Li_xTM_{1-x}O$ in the wide concentration range $x \in (0, \frac{1}{2})$. This gives an excellent opportunity for further investigation of these highly correlated materials by monitoring changes upon doping. Various properties such as magnetic susceptibility, conductivity, and Seebeck and Hall effects have been investigated in the past.[7-10] Very recently a systematic spectroscopic study which included x-ray photoemission spectroscopy (XPS), bremsstrahlung isochromat spectroscopy (BIS), and oxygen 1*s* x-ray absorption spectroscopy (XAS) of $Li_xNi_{1-x}O$ and $Li_xCo_{1-x}O$ has been reported by van Elp *et al.*[11,12] (referred to as VE). Those experimental studies were also complemented by model-Hamiltonian cluster calculations of the electronic structure and the spectral weights for the relevant excitation processes. We recall some of the main conclusions given in VE that are relevant for the discussion below. The first is that the CoO band gap is of an intermediate character between Mott-Hubbard-like and charge-transfer-like and that such a situation persists with Li doping up to the miscibility gap at $x=0.2$. The second conclusion is that the end member $LiCoO_2$ (or $x=0.5$) is an insulator with a gap of 2.7 eV and contains low-spin highly covalent Co^{3+} ions. This is consistent with magnetic susceptibility measurements, as concluded by Bongers.[13] It is also known[3,5,14-16] that in spite of many efforts and significant contributions to the understanding of the electronic structure of CoO and some other late TM monoxides, a one-particle description of their electronic properties based on a band-structure approach within the density-functional theory (not limited only to the local (spin)-density approximation [L(S)DA]) is still not adequate. However, assuming a point of view presented in VE one might expect the one-particle (band-structure) description of the end member $LiCoO_2$ to be reasonably good and complementary to the approaches based on the localized model Hamiltonians. This is because the end member contains Co^{3+} (d^6) low spin and is basically a closed-shell system in its ground state. It was the purpose of this work to explore this possibility.

We have performed the self-consistent band-structure calculation for $LiCoO_2$ with a local (spin)-density approximation to the density functional (DF). A brief description of the method, the details of calculation, and the resulting electronic band structure are reported in Sec. II. In Sec. III the (local) partial density of states [(L)PDOS] were used to calculate XPS, BIS, and oxygen 1*s* XAS spectra. The results of the calculation are compared with the experimental results taken from Refs. 12 and 17. Finally, Sec. IV summarizes our conclusions, which give firm support to the point of view on the electronic structure of $LiCoO_2$ presented in VE.

II. BAND-STRUCTURE CALCULATION

Band-structure calculations were performed by the localized spherical waves (LSW) method[18,19] using the extended basis set option[20,21] in order to describe appropriately also unoccupied electron states in the energy range higher than a few eV above the bottom of the conduction band. The scalar-relativistic Hamiltonian (spin-orbit interaction not included) was used with exchange and correlation effects treated within L(S)DA with (spin-polarized) Hedin-Lundqvist parametrization. During the self-consistent interactions, which included all core electrons, the basis set of augmented spherical waves (SW) for the valence electrons consisted of 4*s*-, 4*p*-, and 3*d*-like functions for Co and 2*s*-, 2*p*-, and 3*d*-like functions for both O and Li. After that, 4*s*- and 4*p*-like SW's on the oxygen site were added to the basis set and unoccupied

eigenstates of the self-consistent potential were recalculated in a much wider energy range.

$LiCoO_2$ has a rhombohedral structure, which belongs to the space group $R\bar{3}m$ (D^5_{3d}). The unit cell, with parameters $a=4.96$ Å and $\alpha=32°58'$, contains only one chemical formula unit, and the atoms occupy the following Wyckoff positions:[22]

Co: $1a(0,0,0)$,

Li: $1b(\frac{1}{2},\frac{1}{2},\frac{1}{2})$,

O: $2c(x,x,x)$ with $x=0.24$.

This structure can be viewed as one derived from the rocksalt structure of undoped CoO where every second plane of Co atoms stacked in (111) direction is replaced by a plane of Li atoms. The resulting layered structure is fully ordered according to the neutron diffraction data (Ref. 12 and references therein).

One can, formally, introduce a rhombohedral unit cell to describe the rocksalt CoO and, as a matter of fact, such a description is necessary in order to account for antiferromagnetic ordering of the second kind below the Néel temperature (disregarding very small tetragonal distortion of the actual antiferromagnetic phase of CoO). Such a unit cell would have parameters $a=5.217$ Å and $\alpha=33°33'$ (assuming $a=4.26$ Å for the cubic cell), with the atoms in the following Wyckoff positions: Co with opposite magnetic moments in $1a$ and $1b$, respectively, and oxygen in $2c$ with $x=0.25$. One can notice that the values of α and x reported for $LiCoO_2$ above are very close to these in the perfect cubic lattice. The lattice parameter a, however, is significantly smaller than that in pure CoO. It was observed [12] that the value of this parameter in the $Li_xCo_{1-x}O$ system is decreasing linearly as the content of Li substituting Co atoms increases up to the miscibility gap at $x=0.2$. The ordered $LiCoO_2$ end member ($x=0.5$) has, however, significantly smaller value of the lattice parameter than one would obtain by extrapolation of this linear trend (see Fig. 12 in Ref. 12). After these few comments upon the structure of the $Li_xCo_{1-x}O$ system we continue to report the details of calculation. To facilitate a space-filling requirement, common for the atomic sphere (AS) approximation approaches, an additional four empty AS's were allocated in the unit cell, two in Wyckoff position $2c$ with $x=0.13$ and the other two also in $2c$ position but with $x=0.38$. The radii of Co, Li, and O were then selected to reflect sizes of relevant ions and the radii of empty AS's were adjusted appropriately. The values used were 1.778, 2.142, 2.313, 1.542, and 1.285 Å for Co, Li, O, and the two (different) empty AS's, respectively. The self-consistent iteration was carried out with 65 **k** points uniformly distributed in an irreducible part of the Brillouin zone (BZ), which is equivalent to 512 points in the whole BZ. Partial density of states (DOS) was obtained by a simple root-sampling technique with the use of 417 **k** points in the irreducible part of the BZ.

Though allowing for a spin-polarized (magnetic) solution and starting from a few different initial distributions of magnetic moments on Co sites, we observed rapid convergence always to the same nonmagnetic ground state. This observation directly supports the point of view presented in VE that due to a much smaller Co-O distance in $LiCoO_2$ than in CoO, a ligand field in a slightly distorted (compressed) CoO_6 octahedron is strong enough to stabilize a Co^{3+} low-spin ground state. This conclusion follows clearly from Fig. 1 where the electronic band structure of $LiCoO_2$ is shown along a cross section through the BZ as defined in Fig. 2. It is easy to recognize a group of very flat bands which originate from t_{2g} and e_g^* levels of the Co^{3+} d^6 configuration placed in the (nearly) octahedral ligand field. The e_g^* bands are empty and separated by a gap of 1.2 eV from full T_{2g} states. Distortion of the octahedral field causes further splitting of the t_{2g} level also at the Γ point. The small dispersion of these bands, which also moves the tops of the valence bands and the bottoms of the conduction bands away from Γ, is due to hybridization of Co $3d$ states with oxygen states. The lower part of the valence states consists of a group of much wider bands (about 6 eV) originating mostly from oxygen $2p$ states.

The amount of oxygen states mixed into Co d states (or vice versa) can be assessed from Fig. 3, which summarizes the contributions of Co, O, and Li to the total DOS. A much more detailed analysis can be made, however, on the basis of Figs. 4(a), 4(b), and 4(c) where local partial DOS's of Co, O, and Li, respectively, are given in the separate panels. First, one may notice that d states of Co and p states of O dominate over all the other contribu-

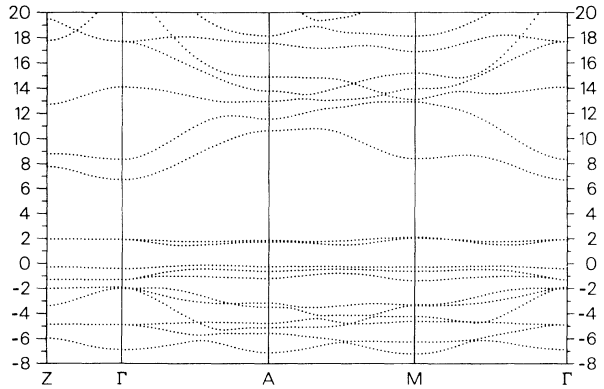

FIG. 1. Electronic band structure of $LiCoO_2$. The tops of the valence bands are set to zero. The definition of cross section through the Brillouin zone is given in Fig. 2.

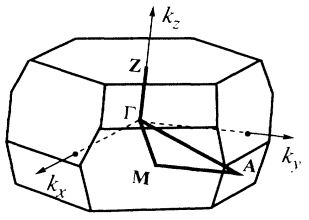

FIG. 2. Brillouin zone of a rhombohedral structure in the case of $LiCoO_2$. The heavy solid line indicates the cross section used for the band-structure plot in Fig. 1.

tions to the valence bands (apart from the narrow band of oxygen 2*s* states at −19 eV, which on the other hand are rather irrelevant for consideration here). Next, by calculating the area (number of states) of the isolated peaks or estimating the area of superimposed features of relevant partial density of states, it is possible to recognize the chemical nature of orbitals contributing to different bands. Though the real symmetry at a Co site is lower it seems to be useful to use O_h point-group representations to label these orbitals.

The diagram which summarizes the results of such analysis is shown in Fig. 5. The height of the blocks gives a realistically estimated width of the bands of different character; therefore the energy scale corresponding to that of the band-structure plot in Fig. 1 and all DOS plots is reproduced on the side of the diagram. To facilitate the comparison with the model-Hamiltonian cluster calculation[12] and just to make this diagram readable, other states of oxygen and all states of lithium, with one exception, are not included. The unoccupied states between 6.5 and 12 eV are dominated by Li *s* and *p* contributions. The Li contribution continues to higher energies. These Li states are shown by the dashed-line block. The numbers within blocks show fractional occupation of bands of different character. The first number gives the fraction of indicated Co states and the second one the fraction of *p* states of oxygen. A deviation from 1 indicates the contribution of all other states that are not included in this simplified diagram. One should have in mind, however, that as for any population analysis, this also suffers from a certain arbitrariness and should be used with caution. In particular the separation of oxygen states within overlapping t_{1u}, e_g, and a_{1g} complexes is less accurate than the total Co and O *p* fractions within that complex, which are equal to 0.18 and 0.75, respectively. Summing up all Co and O *p* contributions in the occupied bands, we obtained the values 0.367 and 0.542 as the fraction of 18 valence electrons. One can derive the total occupation fractions from the results of cluster model-Hamiltonian multiconfiguration calculation given in Ref. 12 (Table VII therein). The respective values are 0.368 and 0.632. The latter numbers add up to 1 in the model calculation because only 3*d* Co and 2*p* O electrons were included. One may notice a remarkably good agreement between these two different approaches.

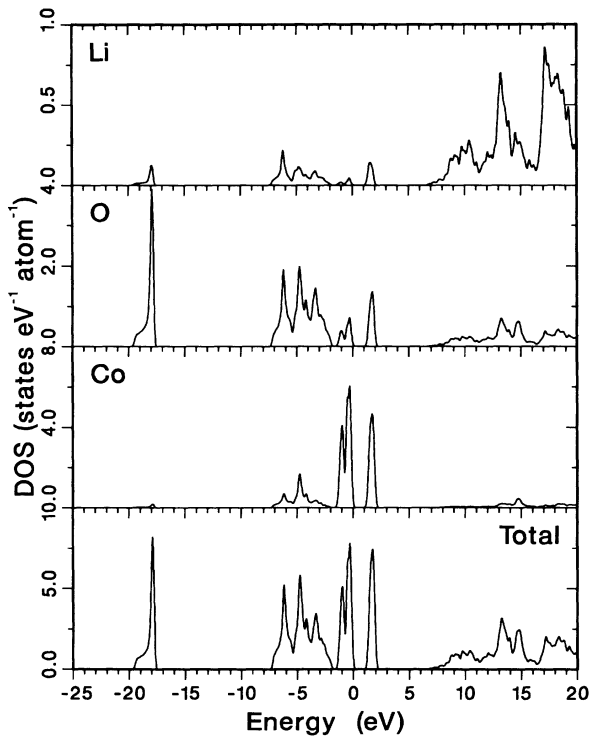

FIG. 3. Density of states of $LiCoO_2$ (bottom panel) together with local density of states on Co, O, and Li sites. In the case of total DOS one should read $(cell)^{-1}$ instead of $(atom)^{-1}$ in the density units description. The top of the valence band is set to zero. Two sharp peaks around the main gap correspond to the flat bands (see Fig. 1) originating from t_{2g} and e_g^* Co *d* states. Gaussian broadening with the FWHM equal to 0.1 eV was used.

We would like to point out that in the simplified diagrams of molecular orbitals in an octahedral field when one considers only *p* ligand orbitals, the t_{2g} level remains nonbonding. Here however, because of the presence of other oxygen states, lithium states, lower than O_h point symmetry, and finally because of translational invariance, we found bands emerging from t_{2g} orbitals to be bonding with a significant level of covalency. A much higher level of covalency was found, of course, in e_g bonding states which are placed in the center of the 6-eV-wide oxygen *p*-dominated band. It is also an important observation that the fraction of oxygen states in the antibonding e_g^* band, just above the gap, is as much as two times higher than that at the top of the valence band (t_{2g}).

Finally, we will close this section with a comment about the value of the gap obtained within the density-functional calculation. It is well known that *normal* error of the L(S)DA in reproducing a gap in the wideband systems is about 30–40% (e.g., in *classical* IV, III-V, or II-VI semiconductors). It is also known that the self-interaction error of the L(S)DA increases when the orbitals involved become more localized. This is one of the reasons leading to the collapse of a one-particle description based on the L(S)DA in the narrow-band systems. The gap obtained here for $LiCoO_2$ (as mentioned already above) is equal to 1.2 eV while it was estimated experimentally[12] to be equal to 2.7±0.3 eV. This gives an error of (55±5)%, which we find very reasonable.

III. SPECTROSCOPY: XPS, BIS, AND XAS

Local partial DOS's of $LiCoO_2$ presented in Fig. 4 were used to calculate a valence x-ray photoemission spectrum, bremsstrahlung isochromat spectrum, and oxygen 1*s* x-ray absorption spectrum. To account for lifetime and instrumental-broadening effects, the relevant partial DOS's were convoluted with Lorentzian and Gaussian distributions, respectively. The parameters we used here are reported in Table I.

We start with the valence XPS. In the upper panel of Fig. 6 we show the spectrum obtained simply from the total DOS of $LiCoO_2$. In the middle panel we present spec-

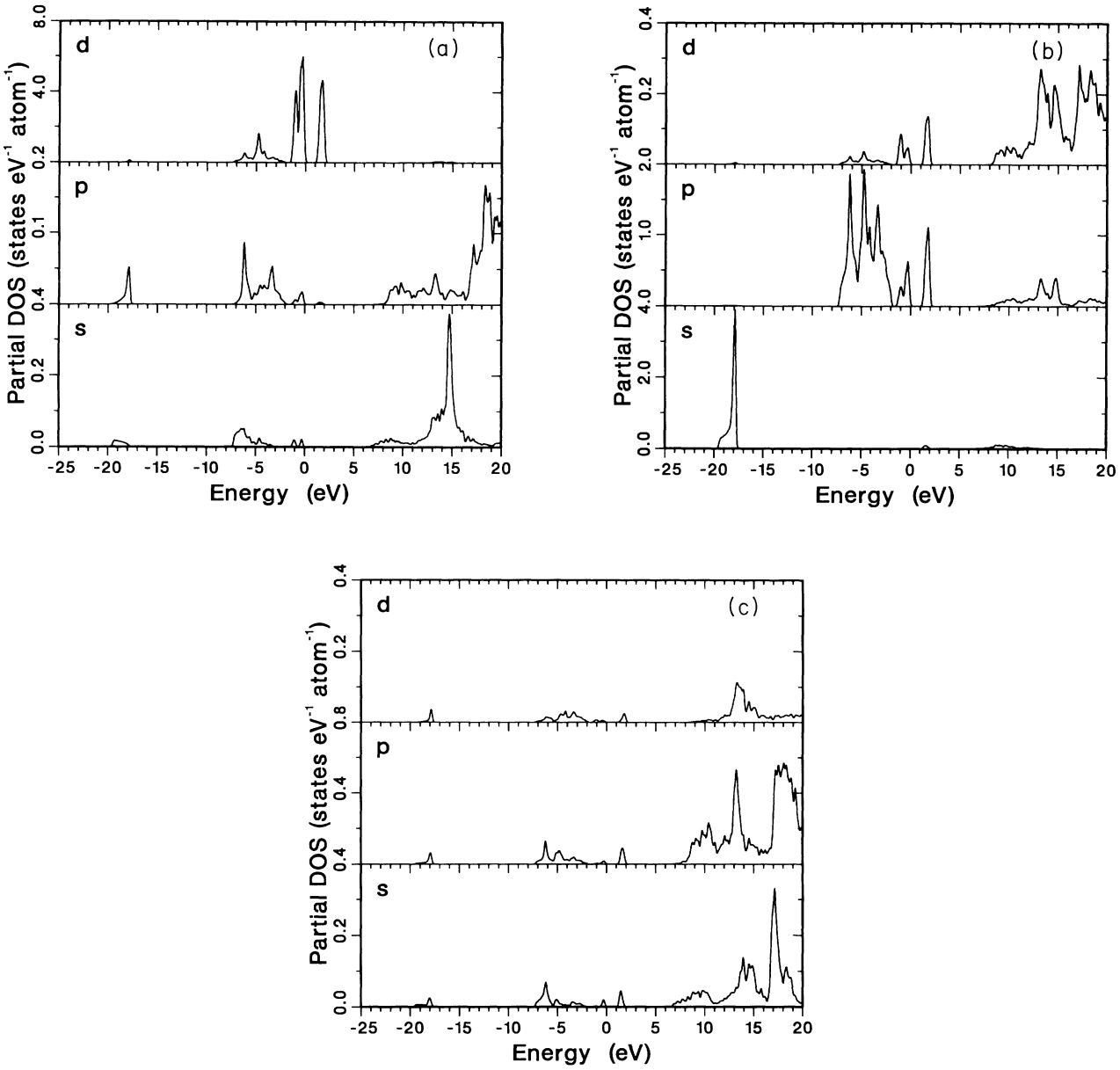

FIG. 4. Partial local DOS of (a) Co, (b) O, and (c) Li in $LiCoO_2$. Top of the valence band is set to zero. When comparing contributions of states with different character note the different scale of some panels.

TABLE I. Broadening parameters used in convolution of local partial DOS. The linear term, accounting for the lifetime of a conduction or valence hole, is a purely empirical value based on previous experience (see, e.g., references in Ref. 26). Instrumental broadening as reported by VE. FWHM denotes full width at half maximum.

	Lorentzian FWHM (eV)	Gaussian FWHM (eV)
Valence XPS	$0.5+0.09(E-E_0)$	1.0
BIS	$0.5+0.10(E-E_0)$	0.8
Oxygen K XAS	$0.4+0.10(E-E_0)$	0.5

TABLE II. Relative photoionization cross sections of the valence electrons for x-ray energy equal to 1254 eV (Mg $K\alpha$ line). All entries were normalized to the value for 3d Co.

		As taken from Ref. 23	Optimized
Co	3d	1.00	1.00
	4s	0.14	0.42
	4p		0.42
O	2s	0.435	1.35
	2p	0.075	0.225

trum calculated by weighting local partial states of Co and O by the atomic photoionization cross sections for a photon energy of 1253.6 eV (Mg, $K\alpha$ line) taken from Ref. 23 (the contribution of Li is negligible). Finally, the lower panel gives the results we obtained by optimization of the weighting factors. Both sets of values we used are listed in Table II. In all three cases a background of the form $A\int_{+\infty}^{E} I(E)dE$ was added, where $I(E)$ stands for the spectrum without background and the factors A were adjusted, yielding values 0.35, 0.75, and 0.7, respectively. In all cases the experimental spectrum taken from Ref. 12 is given for comparison.

The purpose of this procedure is to show the limitation of the one-particle description based on the (local) density-functional theory. It is well established that closed-shell atomic orbital eigenenergies of the Kohn-Sham equation interpreted as the electron removal energies give systematically too low values[24] (contrary to Hartree-Fock giving always too high values for the removal energies). This is why the peak originating from oxygen 2s states appears at -18.1 eV, misplaced by 2.3 eV [compare Fig. 4(b)].

On the other hand, a satellite structure ranging from -9 to -14 eV has no explanation based on the density-functional band-structure calculation. It arises from the presence of an unscreened or at least *poorly* screened Co 3d excess hole. Such a hole remains localized, which breaks the translation symmetry and thus goes beyond the band-theory picture. A proper description of the satellites in photoemission would require a dynamic (many-body) response theory, unfortunately never formulated to the level of successful application in realistic systems. However, a rather successful description of the satellite structure in the electron-removal spectral weight in $LiCoO_2$ and CoO was obtained by a multiconfiguration model-Hamiltonian cluster calculation (see Ref. 12 and references therein). Having explained the origin of differences we stress good overall agreement between calculated and measured valence XPS spectra. Our understanding of the electronic structure of $LiCoO_2$ is consistent with that presented in VE.

In the next step, we compare, in Fig. 7, the BIS experimental result with the calculation based on the local partial DOS given in Fig. 4. The BIS measurement was performed using a modified Kratos 200 spectrometer with an Al $K\alpha$ (1486.6 eV) monochromator and a home-built type of Pierce electron gun capable of giving an electron current of about 200 μA. The background pressure was in the 10^{-10} Torr range and the instrumental broadening was estimated to be 0.8 eV. The spectra were taken in several scans and averaged afterwards. In between the scans the sample was scraped *in situ* with a diamond file and checked with XPS.

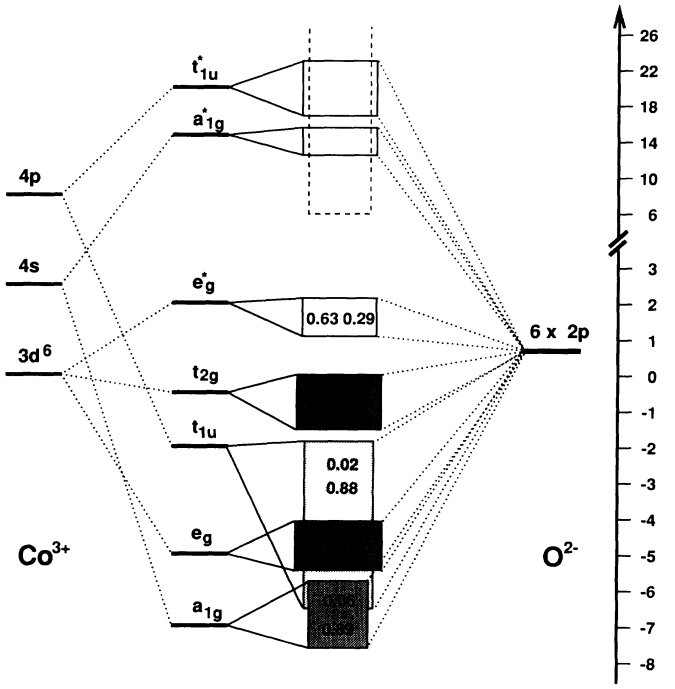

FIG. 5. Diagram of the chemical nature of orbitals contributing to different bands. Occupied states are shaded. The energy scale corresponds to that in Fig. 1. The contribution of Li states indicated by a dashed-line block is included only in the place where it is large. The numbers within blocks give fractional occupation by respective Co states and p states of oxygen. See the main text for more details and discussion.

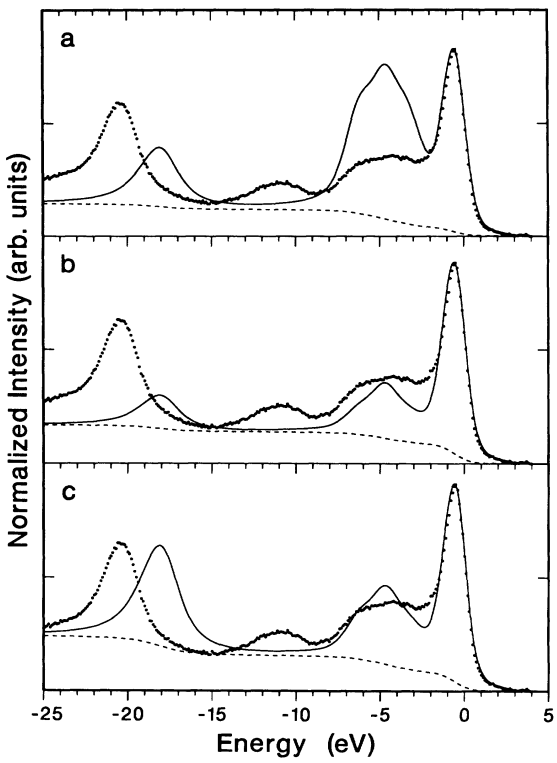

FIG. 6. Valence x-ray photoemission spectrum of $LiCoO_2$. Solid line shows theoretical results (a) obtained from the total DOS; (b) obtained by weighting different local partial DOS's by the photoionization cross sections taken from Ref. 23; (c) obtained by optimizing the weighting factors. For the cases (b) and (c) the weighting factors are listed in Table II. Dashed line represents a calculated background and dots reproduce the experimental data taken from Ref. 12. See the main text for discussion.

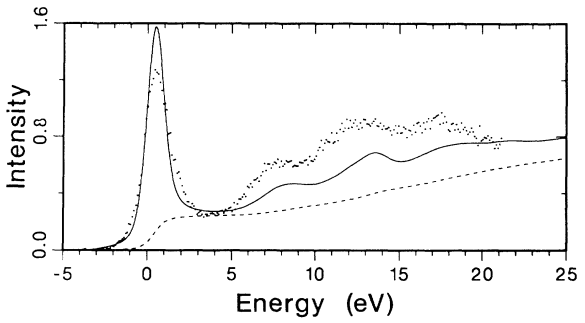

FIG. 7. Bremsstrahlung isochromat spectrum of $LiCoO_2$. Solid line—theoretical spectrum obtained as described in the main text. The background is indicated by the dashed line. Dots—our experimental data.

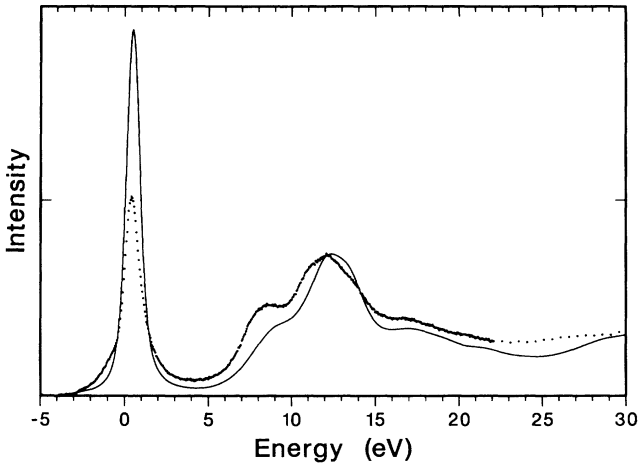

FIG. 8. X-ray absorption K edge of oxygen in $LiCoO_2$. Solid line—calculation, dotted line—experiment (Ref. 17).

The shape of the BIS spectrum is determined by the superposition of all (broadened) local partial DOS's weighted by the appropriate transition matrix elements. (For the broadening parameters, see Table I.) Transition matrix elements were obtained on the basis of an atomic/ionic model calculation[25] for a given kinetic energy of an incoming electron. The procedure was the same as that described in detail in Ref. 21. The relative probabilities of transitions from the continuum to a given atomic function are listed in Table III. The background was added in a similar way as in the case of the XPS spectrum above. The expression $A\int_{-\infty}^{E} I(E)dE$ was used with A set to 1.5. The factor A is the only adjustable parameter used here. Figure 7 shows that the calculated curve reproduces very well all features of our experimental data in the whole energy range. A simple simulation shows, however, that further improvement could be obtained by increasing the relative contribution of oxygen states to the spectrum. In spite of good results obtained before[21] for some transition metals and their alloys using the same approach this may indicate that the transition matrix elements for the BIS process should be calculated with a more realistic model.

Finally, using oxygen partial p density of states [see Fig. 4(b) and Table I for broadening parameters] we obtained the XAS oxygen K edge spectrum and compared it with the experiment[17] in Fig. 8. As in the case of the BIS spectrum above, good agreement in the whole energy range supports the Co^{3+} low-spin state in $LiCoO_2$ as well as the reliability of the extended basis set version of the LSW method in calculations of unoccupied electron states not limited to a few eV above the bottom of the conducting band. It is expected that the effect of the core hole left behind by an electron in the absorption process, when included in the calculation, will further improve the agreement in two ways: first of all, by reduction of intensity of the sharp leading peak, and second, by a shift of some intensity towards lower energy within the broad structure between 6 and 15 eV.[26]

TABLE III. Relative probabilities of transitions from the continuum to given atomic function for kinetic energy of the incoming electrons equal to 1487 eV (Al $K\alpha$) as obtained from Ref. 25. All entries were normalized by the value for 3d Co.

Co		O		Li	
3d	1.00	2s	0.89	2s	0.09
4s	2.00	2p	0.03	2p	0.00
4p	2.06	3s	0.26	3d	0.00
4f	0.00	3p	0.01		
		3d	0.00		

IV. SUMMARY

We performed a self-consistent electronic structure calculation within the L(S)DA for $LiCoO_2$ which is the end member (with $x=0.5$) of the Li-doped $Li_xCo_{1-x}O$ system. A systematic analysis of the resulting band structure and local partial DOS enabled us to construct a molecular bonding diagram (with population analysis) closely resembling Co^{3+} $3d^6$ low-spin ion placed in the octahedral field of oxygen ligands and hybridizing with their 2p orbitals. This result is in full agreement with the result presented in VE. The value of the main gap we obtained here amounts to about 50% of the experimental value reported in VE.

On the basis of the local partial DOS we calculated the valence XPS, BIS, and oxygen 1s XAS spectra. In the case of BIS and XAS we obtained very good agreement with experiment. In the case of the valence XPS spectrum, while preserving overall agreement and consistency we cannot reproduce, however, the structure between -9 and -14 eV. This *satellite* structure results from *poorly* screened 3d Co excess hole and its description goes beyond a one-particle band-structure approach based on the L(S)DA.

Finally, we conclude (consistent with VE) that the interpretation of the electronic structure of $LiCoO_2$ which assumes presence of $3d^6$ low-spin Co^{3+} ions leads to good agreement with a number of experimental results.

ACKNOWLEDGMENTS

This work was supported by the Netherlands Foundation for Chemical Research (SON) and the Netherlands Foundation for Research on Matter (FOM) with financial support from the Netherlands Organization for the Scientific Research (NWO) and the Committee for the European Development of Science and Technology (CODEST) program.

[1]N. F. Mott, Proc. Phys. Soc. London, Sect. A **62**, 416 (1949).
[2]J. Hubbard, Proc. R. Soc. London, Ser. A **277**, 237 (1964); **281**, 401 (1964).
[3]T. Oguchi, K. Terakura, and A. R. Williams, Phys. Rev. B **28**, 6443 (1983).
[4]A. Fujimori and F. Minami, Phys. Rev. B **30**, 957 (1984).
[5]K. Terakura, T. Oguchi, A. Williams, and J. Kübler, Phys. Rev. B **30**, 4734 (1984).
[6]J. Zaanen, G. A. Sawatzky, and J. W. Allen, Phys. Rev. Lett. **55**, 418 (1985).
[7]R. R. Heikes and W. D. Johnston, J. Chem. Phys. **26**, 582 (1957).
[8]W. D. Johnston, R. R. Heikes, and D. Sestrich, J. Phys. Chem. Solids **7**, 1 (1958).
[9]A. J. Bosman and C. Crevecoeur, J. Phys. Chem. Solids **30**, 1151 (1969).
[10]A. J. Bosman and A. J. van Daal, Adv. Phys. **19**, 1 (1970).
[11]J. van Elp, H. Eskes, P. Kuiper, and G. A. Sawatzky, Phys. Rev. B **45**, 1612 (1992).
[12]J. van Elp, J. L. Wieland, H. Eskes, P. Kuiper, G. A. Sawatzky, F. M. F. de Groot, and T. S. Turner, Phys. Rev. B **44**, 6090 (1991).
[13]P. F. Bongers, Ph.D. thesis, University of Leiden, The Netherlands, 1957.
[14]Z.-X. Shen, J. W. Allen, P. A. P. Lindberg, D. S. Dessau, B. O. Wells, A. Borg, W. Ellis, J. S. Kang, and S.-J. Oh, Phys. Rev. B **42**, 1817 (1990).
[15]M. R. Norman, Phys. Rev. Lett. **64**, 1162 (1990); **64**, 2466 (1990).
[16]A. Svane and O. Gunnarsson, Phys. Rev. Lett. **65**, 1148 (1990).
[17]M. Abbate and F. M. F. de Groot (private communication).
[18]The localized spherical wave method of electronic structure calculation is the version of the well-known augmented spherical wave method of Williams *et al.*, Ref. 19. The formalism of the method has been recently described by H. van Keuken, A. Lodder, M. T. Czyżyk, F. Springelkamp, and R. A. de Groot, Phys. Rev. B **41**, 5613 (1990).
[19]A. R. Williams, J. Kübler, and C. D. Gelatt, Jr., Phys. Rev. B **19**, 6094 (1979).
[20]M. T. Czyżyk, R. A. de Groot, G. Dolba, P. Fornasini, A. Kisiel, F. Rocca, and E. Burattini, Phys. Rev. B **39**, 9831 (1990).
[21]M. T. Czyżyk, K. Lawniczak-Jabłońska, and S. Mobilio, Phys. Rev. B **45**, 1581 (1982).
[22]H. J. Orman and P. J. Wiseman, Acta Crystallogr., Sect. C **40**, 12 (1984).
[23]J. J. Yeh and I. Lindau, At. Data Nucl. Data Tables **32**, 1 (1985).
[24]J. P. Perdew and M. R. Norman, Phys. Rev. B **26**, 5445 (1982).
[25]Y. Hahn and D. Rule, J. Phys. B **10**, 2689 (1977).
[26]Such an expectation is based on our previous experience with self-consistent calculations of the core-hole effects on the XAS spectra in semiconductors and metals. See M. T. Czyżyk and R. A. de Groot, in *Proceedings of the Second European Conference on Progress in X-ray Synchrotron Radiation Research, Rome, Italy, 1989*, edited by A. Balerna, E. Bernieri, and S. Mobilio (Italian Physical Society, Bologna, 1990), p. 47; P. J. W. Weijs, M. T. Czyżyk, J. F. van Acker, W. Speier, J. B. Goedkoop, H. van Leuken, H. J. M. Hendrix, R. A. de Groot, G. van der Laan, H. J. Buschow, G. Wiech, and J. C. Fuggle, Phys. Rev. B **41**, 11 899 (1990).

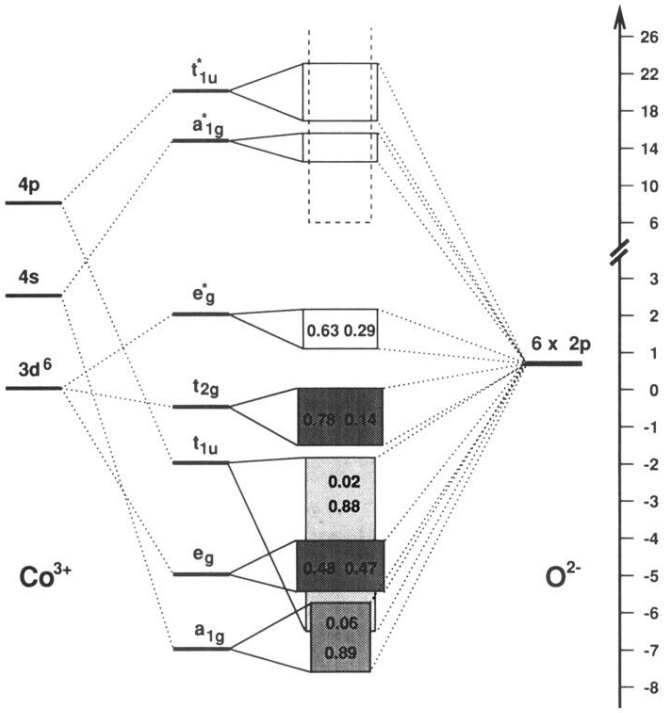

FIG. 5. Diagram of the chemical nature of orbitals contributing to different bands. Occupied states are shaded. The energy scale corresponds to that in Fig. 1. The contribution of Li states indicated by a dashed-line block is included only in the place where it is large. The numbers within blocks give fractional occupation by respective Co states and *p* states of oxygen. See the main text for more details and discussion.